

# Synthesis and Photopolymerization Kinetics of Oxime Ester Photoinitiators

Juan Xu,<sup>1,2</sup> Guiping Ma,<sup>2</sup> Kemin Wang,<sup>1</sup> Juming Gu,<sup>3</sup> Shan Jiang,<sup>1</sup> Jun Nie<sup>2</sup>

<sup>1</sup>School of Materials Science and Engineering, Changzhou University, Changzhou, Jiangsu 213164, People's Republic of China

<sup>2</sup>State Key Laboratory of Chemical Resource Engineering, Beijing University of Chemical Technology, Beijing 100029, People's Republic of China

<sup>3</sup>Institute of Scientific and Technical Information of China, Beijing 100038, People's Republic of China

Received 15 January 2011; accepted 10 March 2011

DOI 10.1002/app.34551

Published online 2 August 2011 in Wiley Online Library (wileyonlinelibrary.com).

**ABSTRACT:** Oxime Ester (OXE) Photoinitiators were synthesized and characterized by HPLC, FTIR, UV-Vis spectra, and <sup>1</sup>H-NMR. The UV-Vis spectra of these photoinitiators were similar to Benzophenone (BP) but showed large red-shifted maximum absorption. OXE were not only soluble in many solvents and (meth) acrylate monomers but also could be dispersed easily in propylene glycol monomethyl ether acetate (PGMEA). The kinetics of polymerization of monomer using OXE as

photoinitiator was studied by Real-time infrared (RTIR) spectra. It showed that OXE were an efficient photoinitiator. The concentration of OXE, functionality of monomer, and light intensity had effect on the photopolymerization kinetics. © 2011 Wiley Periodicals, Inc. *J Appl Polym Sci* 123: 725–731, 2012

**Key words:** oxime ester photoinitiator; photopolymerization; polymerization kinetics; real-time infrared

## INTRODUCTION

Photopolymerization science and technology have assumed an increasing relevance in many applications in the past several decades due to its unique advantages of 5E (efficient, enabling, economical, energy saving, and environmental friendly).<sup>1–3</sup> It is based on the use of photophotoinitiator systems suited to absorb a light to produce primary radical species, which can initiate polymerization. The type I photoinitiators undergo a direct photo fragmentation process ( $\alpha$ - or less common  $\beta$ -cleavage) upon absorption of light. The type II photoinitiators are based on compounds whose triplet excited states readily react with hydrogen donors. Photoinitiators play an essential role in all the photocurable formulations. Great attention has been paid to synthesize new kinds of photoinitiators, which are able to use in different fields such as negative photo-resist,<sup>4,5</sup> liquid crystal displays (LCDs),<sup>6</sup> dental materials,<sup>7</sup> 3D fluorescence imaging,<sup>8</sup> and food beverages<sup>9</sup> in recent years. Some traditional photoinitiators are widely

produced and applied to the field of light-cured materials, such as, benzoin derivatives,  $\alpha,\alpha$ -2-alkoxy phenyl ketones,  $\alpha$ -hydroxy alkyl ketones,  $\alpha$ -amino-alkyl ketones, acyl phosphine oxide, benzophenone/ amines, mikitone, thiophene tons/amine. However, these traditional photoinitiators more or less showed the low-polymerization rate and conversion rate, differential solubility and low transparency, oxygen inhibition and poor stability.

O-acyloxime photoinitiators had been reported in recent year and attracted more and more attentions.<sup>10,11</sup> As our continuous studies on the development of highly efficient photoinitiator systems for the biomolecular photoinitiating system,<sup>12,13</sup> a study of four novel oxime ester photoinitiators which might be applied in other fields is presented in this study. The photoinitiators can absorb light of a particular wavelength from 300 to 400 nm to generate active species, which can convert a crosslinker monomer into a crosslinked network. The carbazole structure group as a substituent on photoinitiator molecules is of our interest because it can not only enhance the solubility of the photoinitiators but also lead to a big red shift of the absorption of the electron-accepting photoinitiator. The stability and sensitive activity of Oxide Ester photoinitiators were improved by the introduction of diphenyl sulfide or carbazole group which had large conjugated system and strong intramolecular electron transfer properties. The designed compounds could generate acids or bases upon irradiation of light, which present a

Correspondence to: J. Nie (niejun@mail.buct.edu.cn).

Contract grant sponsor: Natural Science Foundation of Jiangsu Province; contract grant number: BK2010190.

Contract grant sponsor: Fundamental Research Funds (Central Universities and Changzhou Microelectronics Chemical Material Public Technology Platform).

great interest in the field of polymeric photosensitive systems and are essential component in chemically amplified photoresists. The designed compounds have high thermal stability and extremely higher performance in photosensitivity, making them attractive for possible use in the pigmented system.

In this article, we reported the preparation of the oxime ester initiators, and the structure of photoinitiators was characterized by FTIR, UV-Vis absorption spectra, HPLC, and  $^1\text{H-NMR}$ . High-performance liquid chromatography (HPLC) results showed that their purity were higher than 99.0%. The solubility of OXE photoinitiators in many solvents and monomers was determined. The kinetics for photopolymerization of monomer using OXE as photoinitiators was studied by Real-time infrared (RTIR) spectra.

## EXPERIMENTAL

### Materials

Carbazole, ethyl bromide, diphenyl sulfide, chloride, cyclopentyl C, *N*-ethyl carbazole, amyl nitrite, *o*-methyl chloride, acetyl chloride, hydroxylamine, acetic anhydride, and 4-ethyl bromide were purchased from China National Pharmaceutical Group Corp. (Shanghai, China). Ethanol, methane, petroleum ether, methanol, methylene chloride, aluminum chloride, and triethylamine were obtained from Sino-pharm Group Chemical Reagent Co. (Beijing, China). Other reagents were of analytical grade except as noted. 1,6-Hexanedioldiacrylate (HDDA), tripropylene glycol diacrylate (TPGDA), trimethylolpropane-triacrylate (TMPTA), and trimethylolpropanetrime-thacrylate (TMPTMA) were donated by Sartomer Chemical Co. (Exton, PA).

### Instruments

FTIR spectra were recorded on a Nicolet 5700 instrument (Thermo Electron Corp., Waltham, MA) with KBr plates.

$^1\text{H-NMR}$  spectra were measured on a Bruker AV600 unity spectrometer operated at 600 MHz with TMS as an internal reference, using  $\text{CDCl}_3$  as the solvent.

UV-Vis absorption spectra were recorded on a Hitachi U-3010 UV-Vis spectrophotometer (Hitachi High-Technologies Corp., Tokyo, Japan). A cell path length of 1 cm was employed.

High-performance liquid chromatography (HPLC) was operated on the HPLC-10A instrument (Shimadzu Corp., Tokyo, Japan). The chromatographic conditions were as follows: CLC-ODS column (5  $\mu\text{m}$ , 250 mm  $\times$  4.6 mm) used as the stationary phase, methanol-water (90/10, v/v) as mobile phase with a flow rate of 1.0 mL/min.

### Synthesis of oxide ester photoinitiators

Using carbazole as raw material, four oxime ester photoinitiators were synthesized through series reactions such as instead, asymmetric acylation, oxime, and esterification reaction. The final products were purified with recrystallization.

### Synthesis of OXE-2

The detailed experimental procedures for 1-[9-ethyl-6-(2-methylbenzoyl)-9H-carbazol-3-yl]-ethanone-1-(O-acetyloxime) [OXE-2]<sup>14</sup> was shown in Scheme 1(a). The FTIR and  $^1\text{H-NMR}$  spectra were shown in Figure 1(a), FTIR, (KBr,  $\text{cm}^{-1}$ ), 2940  $\text{cm}^{-1}$ (C-H), 1720  $\text{cm}^{-1}$ (O-C=O), 1670  $\text{cm}^{-1}$ (N-C=O), 1600 ( $-\text{Ar}$ ),  $^1\text{H-NMR}$  ( $\text{CDCl}_3$ , 600 MHz):  $\delta$ 1.47–1.50(3H, t,  $-\text{CH}_3$ ), 2.29(3H, s,  $-\text{CH}_3$ ), 2.36(3H, s,  $-\text{CH}_3$ ), 2.50(3H, s,  $-\text{CH}_3$ ), 4.40–4.48(2H, q,  $-\text{CH}_2-$ ), 7.29–8.12(9H, m,  $-\text{benzene}$ ). HPLC, 99.1%.

### Synthesis of OXE-3

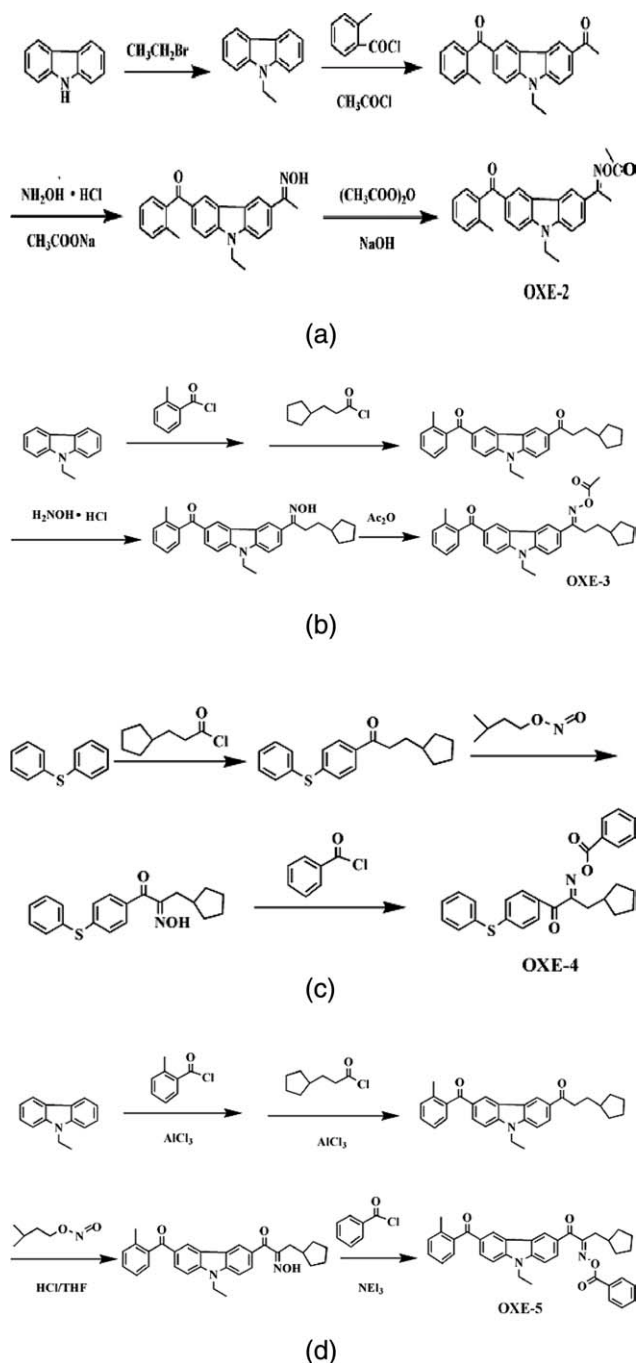
The detailed experimental procedure of 1-diphenyl sulfide-1-cyclopentyl benzyl acetone oxime [OXE-3]<sup>15</sup> was shown in Scheme 1(b). The FTIR and  $^1\text{H-NMR}$  spectra were shown in Figure 1(b), FTIR, (KBr,  $\text{cm}^{-1}$ ), 2925  $\text{cm}^{-1}$ (C-H), 1740  $\text{cm}^{-1}$ (O-C=O), 1620  $\text{cm}^{-1}$ (Ar-C=O), 1595( $-\text{Ar}$ ).  $^1\text{H-NMR}$  ( $\text{CDCl}_3$ , 600 MHz):  $\delta$ 1.13–1.17 (2H, q,  $-\text{CH}_2-$ ), 1.47–1.90(9H, m,  $-\text{cyclopentane}$ ), 2.28 (1H, s,  $-\text{CH}_3$ ), 2.36(1H, s,  $-\text{CH}_3$ ), 2.96–3.00(2H, q,  $-\text{CH}_2-$ ), 4.40–4.44(2H, q,  $-\text{CH}_2-$ ), 7.29–8.55(10H, m,  $-\text{benzene}$ ). HPLC, 99.2%.

### Synthesis of OXE-4

The detailed experimental procedure for 1-diphenyl sulfide-1-cyclopentyl benzyl acetone oxime [OXE-4]<sup>16</sup> was shown in Scheme 1(c). The FTIR and  $^1\text{H-NMR}$  spectra were shown in Figure 1(c), FTIR, (KBr,  $\text{cm}^{-1}$ ): 2930  $\text{cm}^{-1}$ (C-H), 1720  $\text{cm}^{-1}$ (O-C=O), 1635  $\text{cm}^{-1}$ (Ar-C=O), 1605( $-\text{Ar}$ ).  $^1\text{H-NMR}$  ( $\text{CDCl}_3$ , 600 MHz) results was shown as following,  $\delta$ 1.19–2.15(9H, m,  $-\text{cyclopentane}$ ), 3.96–3.00(2H, d,  $-\text{CH}_2-$ ), 7.20–8.10(14H, m,  $-\text{benzene}$ ). HPLC, 99.0%.

### Synthesis of OXE-5

The detailed experimental procedures for 1-(6-*o*-methyl benzoyl-9-ethylcarbazole)-1-cyclopentyl benzyl acetone oxime [OXE-5]<sup>16</sup> was shown in Scheme 1(d). The FTIR and  $^1\text{H-NMR}$  spectra were shown in Figure 1(d), FTIR, (KBr,  $\text{cm}^{-1}$ ): 2920  $\text{cm}^{-1}$ (C-H), 1735  $\text{cm}^{-1}$ (O-C=O), 1630  $\text{cm}^{-1}$ (Ar-C=O), 1600( $-\text{Ar}$ ).  $^1\text{H-NMR}$  ( $\text{CDCl}_3$ , 600 MHz):  $\delta$ 1.27–2.26 (12H, m,  $-\text{cyclopentane}$   $-\text{CH}_3$ ), 2.36 (3H, s,  $-\text{CH}_3$ ),



**Scheme 1** a: Synthesis of OXE-2; b: Synthesis of OXE-3; c: Synthesis of OXE-4; d: Synthesis of OXE-5.

3.05–3.07 (2H, d,  $-\text{CH}_2-$ ), 4.43–4.48 (2H, q,  $-\text{CH}_2-$ ), 7.25–8.95 (15H, m, -benzene). HPLC, 99.2%.

### Solubility

Solubility of OXE photoinitiators in the selected solvents was determined by the following procedure: The compound was gradually added to a solvent (100.0 g), while the mixture was stirred. The com-

pound continued to add to the mixture till to obtain the saturated solution. The solubility of the photoinitiator was determined by measuring the ratio of the soluble photoinitiator with the solvent.

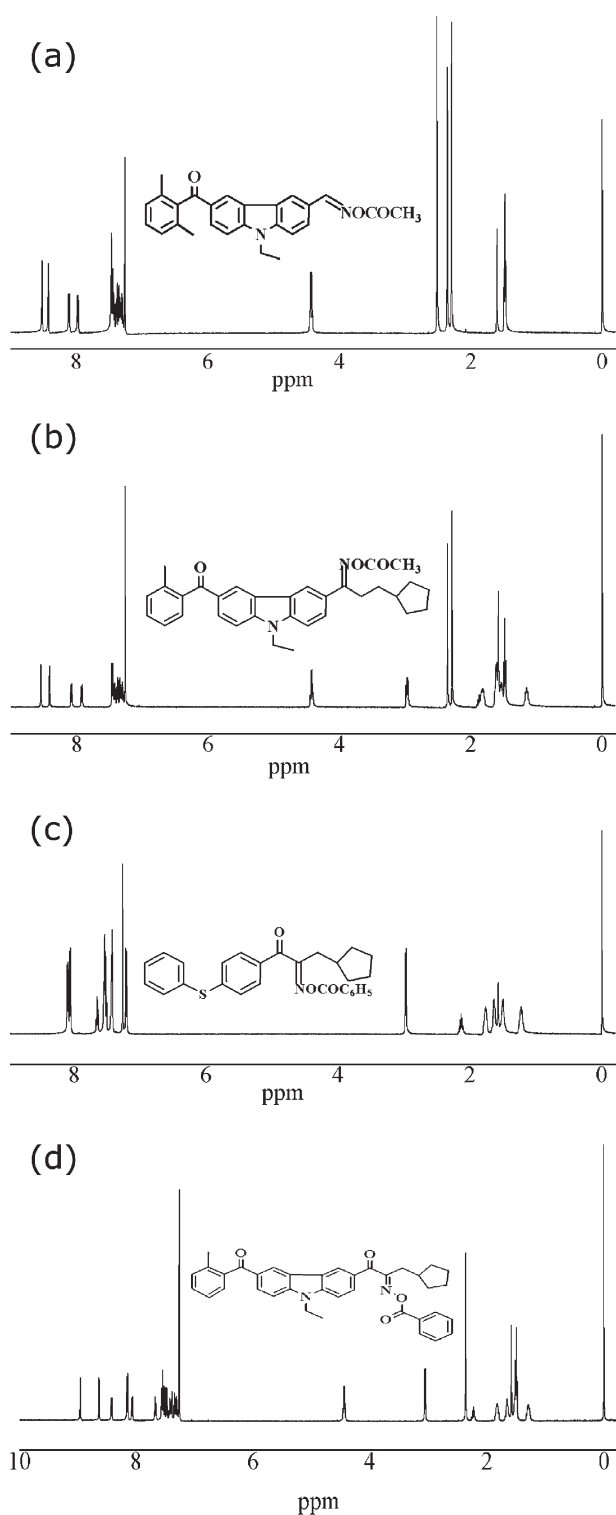


**Figure 1** a:  $^1\text{H-NMR}$  spectrum for OXE-2 in  $\text{CDCl}_3$ . b:  $^1\text{H-NMR}$  spectrum for OXE-3 in  $\text{CDCl}_3$ . c:  $^1\text{H-NMR}$  spectrum for OXE-4 in  $\text{CDCl}_3$ . d:  $^1\text{H-NMR}$  spectrum for OXE-5 in  $\text{CDCl}_3$ .

**TABLE I**  
Solubility of Oxime Ester Photoinitiators

Solubility	OXE-2	OXE-3	OXE-4	OXE-5
PGMEA	2.6	13.0	27.5	16
Cyclohexanone	16.5	26.0	30.0	23
Toluene	12.5	23	28	16
Methanol	21	19	5.8	1.2
Acetonitrile	12	15	9	8
PTGDA	3.6	3.2	4.5	2.9
TMPTA	2.8	3.2	4.4	3.1

### Real-time infrared (RTIR)

Real-time infrared (RTIR) spectra were recorded on a modified Nicolet 5700 spectrometer with a horizontal sample holder (Nicolet 5700, Thermo Electron). Photopolymerizations were conducted in a cell prepared by sandwiching the mixture of photoinitiator and monomer between two glass slides and spacers with  $15 \pm 1$  mm in diameter and  $1.2 \pm 0.1$  mm in thickness. The UV light photopolymerization was triggered by a UV spot light source (EFOS Lite, with 300–420 nm filter and crystal optical fiber that the diameter at the fiber exit was 5 mm, Canada). Real-time FTIR data were collected with the resolution of  $4 \text{ cm}^{-1}$  and 0.3985 s sampling interval. The absorbance change of  $=\text{C}-\text{H}$  peak area from  $6101$  to  $6261 \text{ cm}^{-1}$  in the near IR range was correlated to the extent of polymerization. For each sample, the series FTIR runs were repeated three times and the error on the reported double bond conversion as a function of polymerization time was less than 1%. The degree of double conversion (DC) of the function groups could be calculated by measuring the peak area at each time of the reaction and determined by the following equation.<sup>17</sup> The rate of polymerization ( $R_p$ ) could be determined from the differential of curve of conversion versus irradiation time.<sup>18</sup>

$$\text{DC} = [(A_0 - A_t)/A_0] \times 100$$

where DC was the conversion at  $t$  time,  $A_0$  and  $A_t$  were the peak area of function group before irradiation and at  $t$  time.

## RESULTS AND DISCUSSION

### Solubility of photoinitiator

Solubility in organic solvents of oxime ester photoinitiators is one of the most important parameters in practical application. The solubility of oxime ester photoinitiators in different organic solvents and acrylate monomers was summarized in Table I. Oxide Ester photoinitiator exhibited good solubility in non-polar and polar solvents such as methanol, cyclohexanone, benzene, acetonitrile, and dimethylformamide

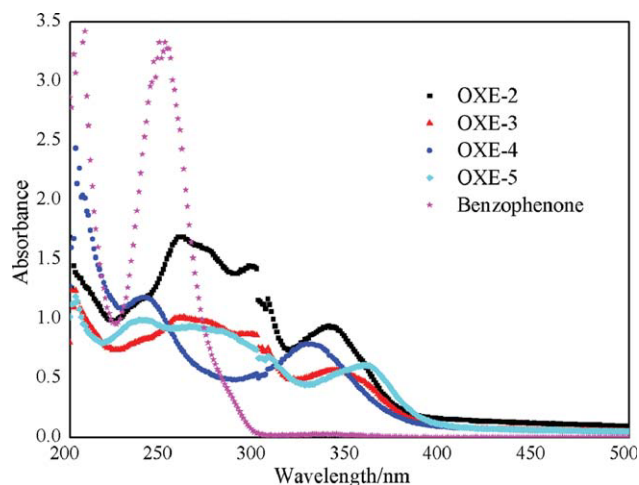


**Figure 2** UV-Absorption spectra of photoinitiators in acetonitrile at concentration of  $2 \times 10^{-5} \text{ g/mL}$  in air. [Color figure can be viewed in the online issue, which is available at [wileyonlinelibrary.com](http://wileyonlinelibrary.com).]

(DMF). Particularly, they possessed very good compatibility with commercial difunctional monomer PTGDA and trifunctional monomer TMPTA, which led to expand their business scope and improve application value. The photoinitiators OXE-3, OXE-4, and OXE-5 could dissolve soluble in the common solvents such as acetone and toluene and were highly soluble in the cyclohexanone and propylene glycol monomethyl ether acetate (PGMEA).

### Absorption properties

UV-Vis absorption spectra of oxide ester photoinitiators in acetonitrile were shown in Figure 2. Values for the molar extinction coefficient ( $\epsilon_{\text{max}}$ ) and the wavelength of maximum absorption ( $\lambda_{\text{max}}$ ) were summarized in Table II. According to Figure 2 and Table II, it could be seen that the absorption characteristics of OXE-2, OXE-3, OXE-4, and OXE-5 were different from the benzophenone (BP) which showed the longest wavelength absorption maximum around 253 nm. The maximum of absorption ( $\lambda_{\text{max}}$ ) of OXE-2, OXE-3, OXE-4, and OXE-5, however, were significantly red shifted to 336, 337, 331, and 358 nm, respectively. The high-molar extinction coefficient

**TABLE II**  
Absorption Properties of OXE-2, OXE-3, OXE-4, OXE-5, and Benzophenone in Acetonitrile Solution with the Concentration of  $2 \times 10^{-5} \text{ g/mL}$

Photoinitiator	$\lambda_{\text{max}}$ (nm)	$\epsilon_{\text{max}}$ ( $\text{g}^{-1} \text{ cm}^{-1} \text{ L}$ )
OXE-2	336	67.8
OXE-3	337	34.2
OXE-4	331	59.5
OXE-5	358	62.7
Benzophenone	253	93.7

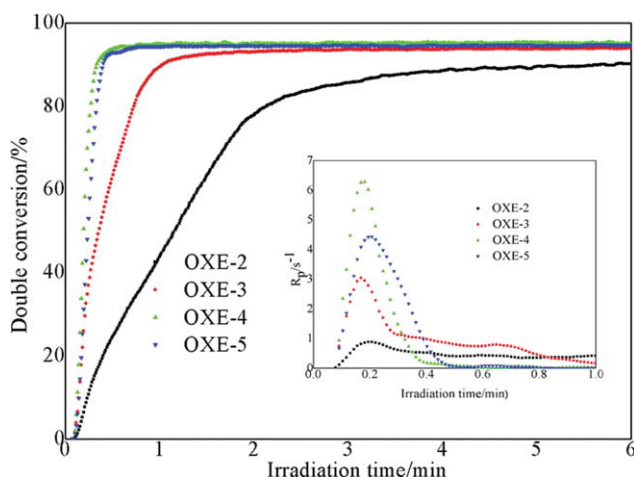


**Figure 3** Effect of different photoinitiator on polymerization of HDDA ( $[OXE] = 0.3 \text{ wt } \%$ ,  $I = 30 \text{ mW/cm}^2$ ). [Color figure can be viewed in the online issue, which is available at [wileyonlinelibrary.com](http://wileyonlinelibrary.com).]

makes OXE an attractive photoinitiator. The transitions in the region of 300–400 nm are usually found owing to the spin forbidden transitions,<sup>19,20</sup> which are well known to attribute to the main benzenoid  $\pi-\pi^*$  type transitions. The significantly red-shifted absorptions indicate that these photoinitiators can be the potential efficient photoinitiators, because they could absorb longer wavelength light effectively than BP at used UV source, thus more free radicals could be produced and higher cure speed than BP could be obtained in the same condition. OXE-2 has an absorption peak at 336 nm and the tailing of the absorption edge is much expanded compared with OXE-3, OXE-4, and OXE-5. From the absorption properties, the photoinitiators are nicely matched with UV source.

### Effect of different photoinitiator on polymerization

Polymerization behaviors of HDDA initiated by four photoinitiators were shown in Figure 3. The final conversions of HDDA polymerization initiated by OXE-3, OXE-4, and OXE-5 could get 96%, and the maximum polymerization rates were reached within 0.2 min. The results indicated that OXE-4 and OXE-5 were the most efficient photoinitiators for the polymerization of HDDA. This could be attributed to that the photoinitiator was high sensitive by the introduction of diphenyl sulfide and carbazole group which had large conjugated system and strong intramolecular electron transfer properties. On the other hand, they contained aromatic molecular structure and were the high efficient photobase agent. When the light exposed, they would release carbon dioxide, which ultimately lead to the formation of the high efficiency of amine.

### Effect of concentration of photoinitiator on polymerization

The concentration of the photoinitiator is a key factor to affect the photopolymerization kinetics.<sup>21,22</sup> To investigate the relationship of conversion and polymerization rate with different concentrations of photoinitiator, real time FTIR was used to determine the extent of DC as a function of time. During irradiation, the decrease of the  $=C-H$  absorption peak area could reflect the extent of polymerization since the absorption of the peak area is proportional to the amount of polymerized  $=C-H$ .<sup>23</sup> The rate of polymerization could be calculated by the time derivative of the DC, accordingly. The plots of conversion and polymerization rate versus irradiation time of HDDA in the presence of different concentrations of OXE-4 were shown in Figure 4. The rate of polymerization could get the maximum value around the 0.2 min period of inhibition time and the conversions of HDDA reached over 92% after irradiated for 1.2 min and the final conversion reached to 97% after irradiated for 10 min. The higher the OXE-4 concentrations, the higher the rate of polymerization was. It might be attributed to the formation of more free radicals with the increasing photoinitiator concentration during irradiation. An optimum photoinitiator concentration was obtained at 0.5 wt %. When the concentration of OXE-4 was more than 0.5 wt %, the rate of polymerization began to decrease because light screening effect of the initiator itself and its photolysis products.<sup>24</sup> The proper initiator concentration for HDDA should lie between 0.3 and 0.5 wt % in the further study from both initiating ability and cost point of view.

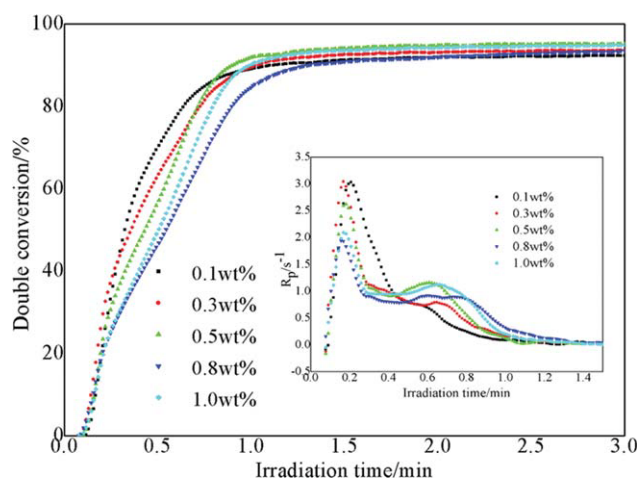


**Figure 4** Effect of OXE-4 concentration on the polymerization of HDDA ( $I = 30 \text{ mW/cm}^2$ ). [Color figure can be viewed in the online issue, which is available at [wileyonlinelibrary.com](http://wileyonlinelibrary.com).]

### Effect of light intensity on polymerization

The light intensity is an important factor for photopolymerization kinetic. Generally, the active species concentration associated with light intensity, the polymerization rate is proportional to the square root of the intensity of the incident UV light.<sup>25</sup> Figure 5 showed the degree of double bond conversion and rate of polymerization versus time plots of HDDA initiated by 0.3 wt % OXE-3 at different light intensity. The polymerization rate increased nearly tripled with increase in light intensity from 10 to 50 mW/cm<sup>2</sup> and the final conversion increased accordingly. The result was according with the previous report that the relationship between proportionality of  $R_p$  to  $I_0^{0.5}$ ,<sup>25</sup> because the higher light intensity could yield more radicals which led to the increase in final double bond conversion and polymerization rate. Moreover, the induction period was decreased by the radicals yielded from increase of light intensity which could overcome oxygen inhibition.<sup>26</sup> When the light intensity increased to 80 mW/cm<sup>2</sup>, the conversion and rate of polymerization were slightly decreased. This indicated that over-dose UV irradiation had an adverse effect on the photopolymerization. It might be due to the combination between free radicals and chain transfer resulted from high light intensity.

### Effect of monomers on polymerization

The effects of monomers on polymerization initiated by 0.3 wt % OXE-5 were shown in Figure 6. The results verified photoinitiators could efficiently initiate the photopolymerization of difunctional and trifunctional monomers, but the behaviors of difunc-

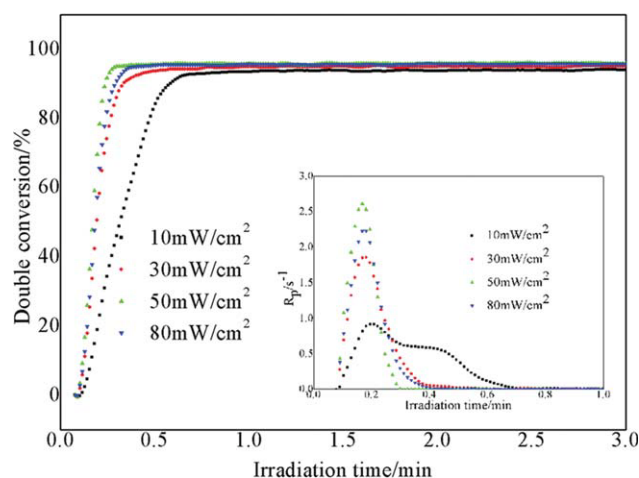


**Figure 5** Effect of light intensity on polymerization of HDDA ([OXE-3] = 0.3 wt %). [Color figure can be viewed in the online issue, which is available at [wileyonlinelibrary.com](http://wileyonlinelibrary.com).]

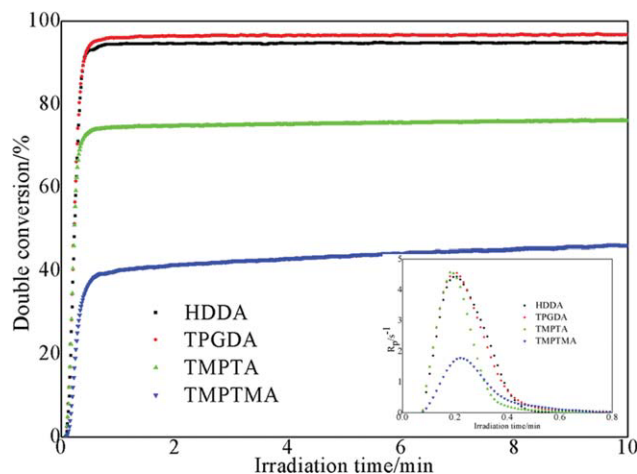


**Figure 6** Effect of monomers functionally on polymerization initiated by OXE-5 ([OXE-5] = 0.3 wt %,  $I = 30$  mW/cm<sup>2</sup>). [Color figure can be viewed in the online issue, which is available at [wileyonlinelibrary.com](http://wileyonlinelibrary.com).]

tional monomers appeared differently from the other trifunctional monomers. The conversion of difunctional monomer was higher than that of TMPTA monomer, but the polymerization rate was lower than it. The polymerization of TMPTA was a very rapid process, in which gelation often occurred at the early stage of polymerization. The formation of such gel structure might restrict the diffusion and mobility of radicals, thus resulting in a very short time to reach the maximum polymerization rate.<sup>27,28</sup> The viscosity of TMPTA was high, thus leading to very high crosslinking density in the whole polymerization process but the final conversion and rate of polymerization of TMPTMA was lower than them, this maybe because of the steric hindrance of methyl group in the molecular structure which hindered itself polymerization.

### CONCLUSIONS

In this article, four kinds of OXE photoinitiators were synthesized which were efficient photoinitiators for free radical polymerization. OXE could dissolve in many solvents and could be dispersed easily in (meth) acrylate monomers. They had significantly long wavelength absorption that afforded efficient light absorption and generated highly reactive radicals with high efficiency. The higher the OXE-4 concentration, the more the free radicals could be produced during irradiation resulting in the higher rate of polymerization. The polymerization rate was proportional to the square root of the intensity of the incident UV light. The conversion of difunctional monomer was higher than that of multifunctional monomer photopolymerization.

**References**

1. Fouassier, J. P. *Photoinitiation, Photopolymerization and Photocuring: Fundamental and Applications*; Hanser: New York, 1995.
2. Allen, N. S.; Marin, M. C.; Edge, M.; Davies, D. W.; Garrett, J.; Jones, F.; Navaratnam, S.; Parsons, B. J. *J Photochem Photobiol A Chem* 1999, 126, 135.
3. He, H. Y.; Li, L.; James, L. *Polymer* 2006, 47, 1612.
4. Sun, L. D.; Jiang, X. S.; Yin, J. *Prog Org Coat* 2010, 67, 225.
5. Li, S. J.; Wu, F. P.; Wang, E. *J Polym* 2009, 50, 3932.
6. Kurt, D.; Tunja, J.; Johannes, B.; Hisatoshi, K.; Akira, M.; Hidetaka, O.; Daniela, H.; Georg, G.; Günther, R. *Macromol Symp* 2004, 217, 77.
7. Shi, S. Q.; Nie, J. *Dent Mater* 2008, 24, 530.
8. Zhang, X.; Sun, Y. M.; Yua, X. Q.; Zhang, B. Q.; Huang, B. B.; Jiang, M. H. *Synth Met* 2009, 159, 2491.
9. Gianni, S.; Giovanni, C.; Gloria, C.; Dario, G.; Massimo, R.; Rosaria, V.; Zuo, Y. T.; Sauro, V. *J Chromatogr A* 2008, 1194, 213.
10. Lalevée, J.; Allonas, X.; Fouassier, J. P.; Tachi, H.; Izumitani, A.; Shirai, M.; Tsunooka, M. *J Photochem Photobiol A Chem* 2002, 151, 27.
11. Mallavia, R.; Sastre, R.; Amat-Guerri, F. *J Photochem Photobiol A* 2001, 138, 193.
12. Wang, K. M.; Nie, J. *J Photochem Photobiol A* 2009, 204, 7.
13. Shi, S. Q.; Xiao, P.; Wang, K. M.; Gong, Y. K.; Nie, J. *Acta Mater* 2010, 6, 3067.
14. Kunimoto, K.; Tanabe, J.; Kura, H.; Oka, H.; Ohwa, M. *Radtech Report May/June 2004*, 30.
15. Qian, X. C.; Wang, B.; Wu, S. M. CN. Pat. CN101508744 (2009).
16. Qian, X. C.; Wang, B.; Ding, Z. C. CN. Pat. CN101565472 (2009).
17. Decker, C.; Nguyen, T.; Viet, T.; Thi, H. P. *Polym Int* 2001, 50, 986.
18. Decker, C.; Moussa, K. *Macromolecules* 1989, 22, 4455.
19. Robert, L. *J Polym Sci Part A: Polym Chem* 2002, 40, 1504.
20. Sigrid, J.; Robert, L. *Macromol Rapid Commun* 2005, 26, 1687.
21. Li, S. J.; He, Y.; Nie, J. *J Photochem Photobiol A* 2007, 191, 25.
22. Shi, S. Q.; Gao, H.; Wu, G. Q.; Nie, J. *Polymer* 2007, 48, 2860.
23. Wang, K. M.; Yang, D. Z.; Xiao, M.; Chen, X. M.; Lu, F. M.; Nie, J. *Acta Biomater* 2009, 5, 2508.
24. Musanje, L.; Ferracane, J. L.; Sakaguchi, R. L. *Dent Mater* 2009, 25, 994.
25. Lecamp, L.; Youssef, B.; Bunel, C.; Lebaudy, P. *Polymer* 1997, 38, 6089.
26. Tom, S.; Ulrich, D. *Radiat Phys Chem* 1999, 55, 615.
27. Jiang, X. S.; Xu, H. J.; Yin, J. *Polymer* 2004, 45, 133.
28. Wang, H. Y.; Wei, J.; Jiang, X. S.; Yin, J. *J Photochem Photobiol A* 2007, 186, 106.